

1 **Supporting Information**

2

3 **Green reaction engineering towards iron-based nanostructured hybrid as an electrocatalyst**
4 **for oxygen evolution reaction**

5

6 Anna G. Dymerska^{a*}, Karolina Wenelska^a, Farit Vagizov^b, Almaz L. Zinnatullin^b, Rustem
7 Zairov^{c,d}, Ewa Mijowska^{a*}

8

9 a. Department of Nanomaterials Physicochemistry, Faculty of Chemical Technology and
10 Engineering,

11 West Pomeranian University of Technology, Szczecin, Piastów Ave. 42, 71-065 Szczecin, Poland.

12 b. Institute of Physics, Kazan Federal University, Kremlyovskaya 18, 420008 Kazan, Russia

13 c. A. M. Butlerov Institute of Chemistry, Kazan Federal University, Kazan, 420008, 1/29
14 Lobachevskogo

15 str., Russian Federation

16 d. Arbuzov Institute of Organic and Physical Chemistry, FRC Kazan Scientific Center, Russian
17 Academy

18 of Sciences, 420088, Arbuzov str. 8, Kazan, Russian Federation

19

20 *Corresponding authors:

21 Anna G. Dymerska: anna.dymerska@zut.edu.pl

22 Ewa Mijowska: ewa.mijowska@zut.edu.pl

Microscopic analysis

Scanning transmission electron microscopy (STEM) was used with energy-dispersive X-ray spectroscopy (EDS) to yield a comprehensive insight into the elemental composition and distribution within the samples. STEM-EDS analyses were performed on pristine Fe/Ni and Fe/Ni_450C (**Figure S1**). As illustrated in **Figure S1(A, B)**, the flakes were discerned to comprise an inner Fe layer segregated from an outer Ni layer by O elements. At the same time, the flower-like structures exhibited the converse arrangement, featuring Ni elements positioned above Fe, interspersed with oxygen. However, following reduction at 450 °C (**Figure S1(C, D)**), the material exhibited a surface predominantly covered by Ni, with O element between Fe-core regions, thus the same transverse elemental distribution as the flake regions in the initial sample.

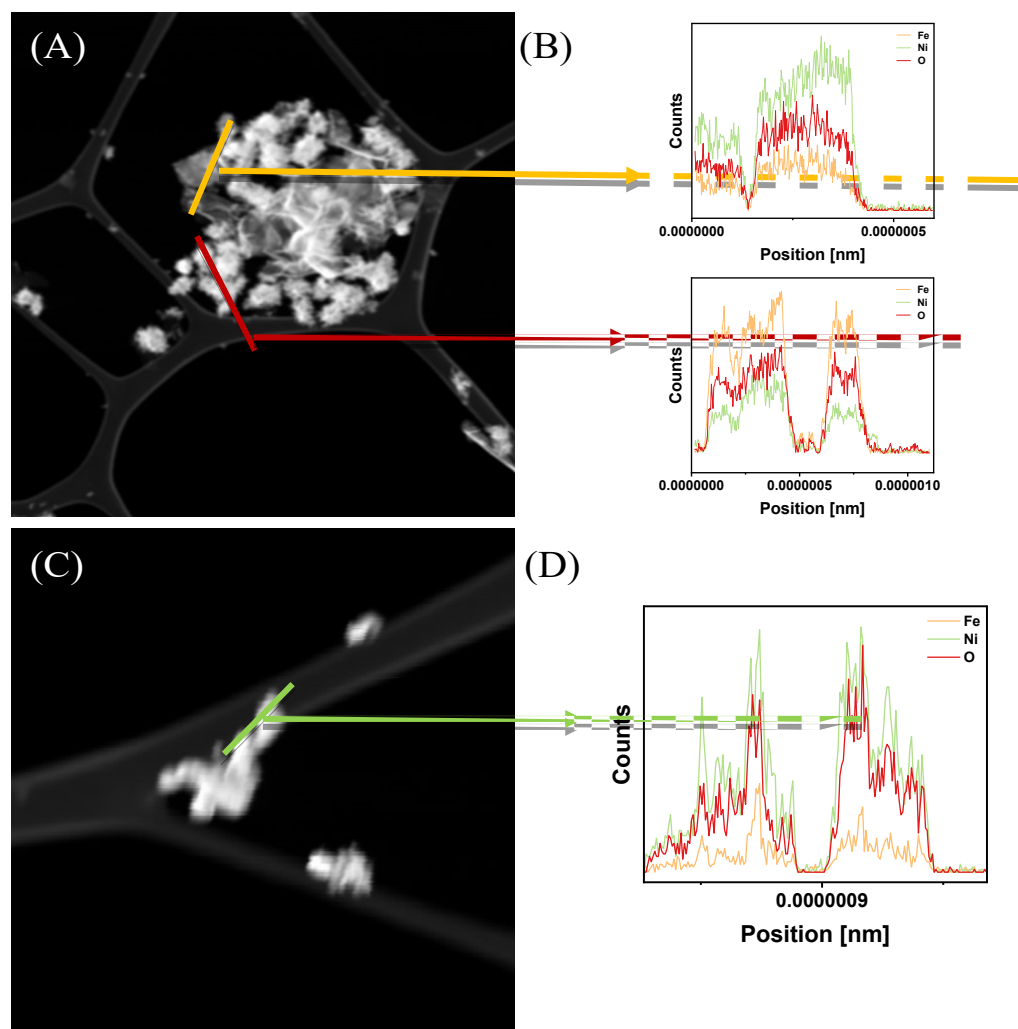


Figure S1. STEM images with EDS line profile of (A-B) the initial Fe/Ni sample, and (C-D) Fe/Ni_450C.

X-Ray Diffractometry

1- $(\text{H}_3\text{O})_{0.66}\text{NiO}_2(\text{H}_2\text{O})_{0.24}$, 2- NiFe_2O_4 , 3- Fe_3O_4 , 4- Fe_2O_3 ,
5- $(\text{Fe}_{0.67}\text{Ni}_{0.33})\text{OOH}$, (6- $\text{Ni}_3\text{O}_2(\text{OH})_4$, 7- Fe_3C , 8- FeNi_3 , 9- Fe , 10- FeNi)

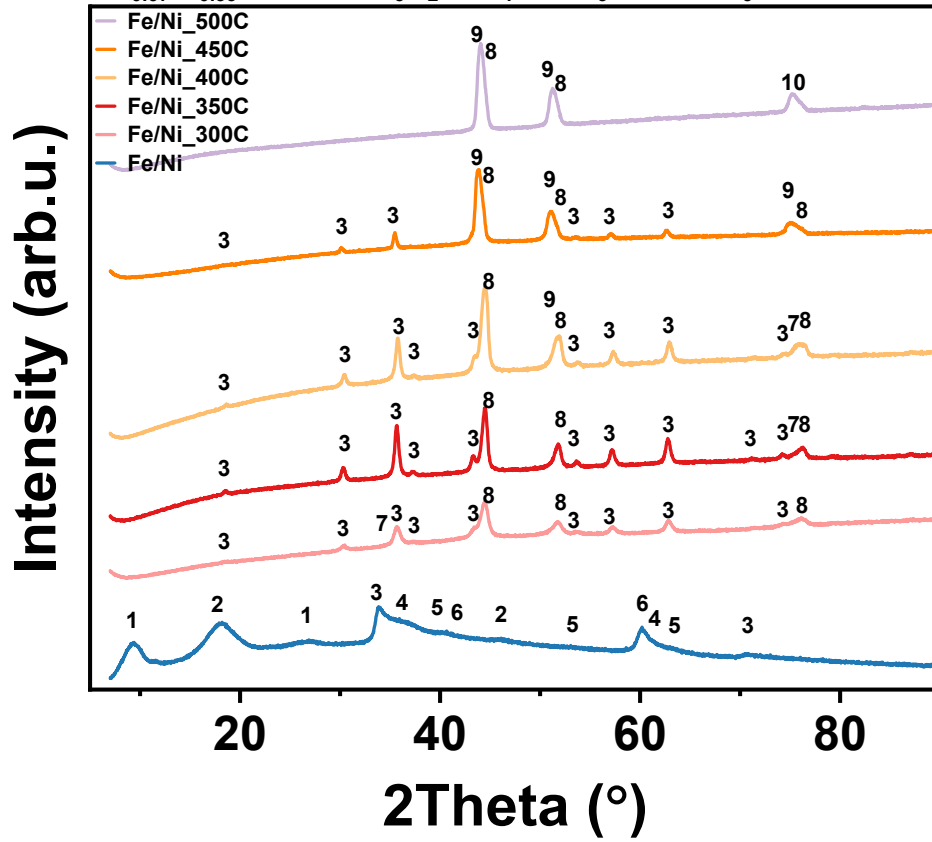


Figure S2. XRD diffractograms of Fe/Ni-based samples.

Ex-situ microscopic analysis

Employing STEM in conjunction with EDS yielded in-depth insights into the composition of these flakes. The analysis unveiled an internal structure comprising iron (Fe), an intermediate layer predominantly composed of oxygen (O), and an outer covering predominantly composed of nickel (Ni) (refer to Figure S3).

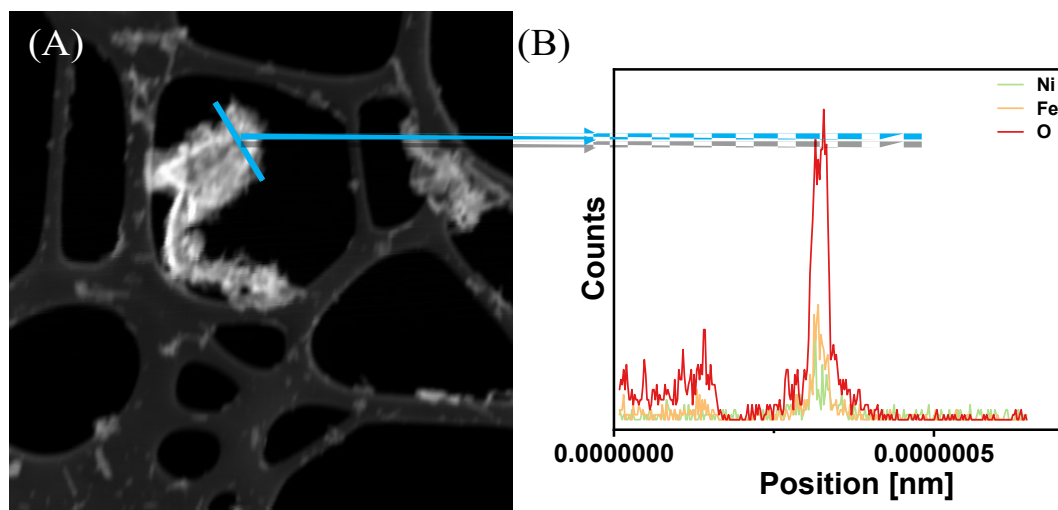


Figure S3. (A) STEM image with (B) EDS line scan of Fe/Ni_{450C} after electrochemical reaction.

X-Ray Photoelectron Spectroscopy

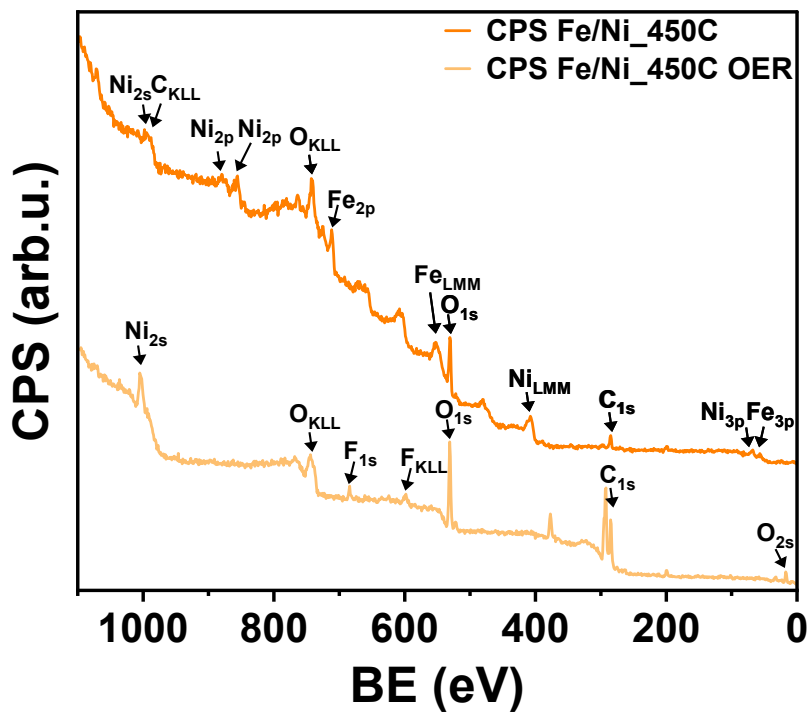


Figure S4. Overview X-Ray spectroscopy of Fe/Ni_{450C} before and after electrochemical reaction.

Comparison of electrochemical properties

Table S1. Comparison of overpotentials, Tafel slopes, and stability of Fe/Ni_450C with leading Fe/Ni-based catalysts reported recently in the literature.

Sample	η [mV]	TS [mV/dec]	stability	Ref.
Fe/Ni_450C	307	42	Eret= 98% (50 mA/cm ²) Deg= 7.14 mV/h	This work
Fe ₂₀ Ni ₈₀	313	62	Deg= 17.2 μ V/h (at 10 mA/cm ²)	S1
Fe ₃ O ₄ -vac	353	50	The exact numerical values are not provided.	S2
Fe/Fe ₂ O ₃ @Fe-N-C-1000a	460	78	Jret= 93.77% (-0.35 V vs. AgCl)	S3
Fe ₂ O ₄ /CC	326	170	Eret= 94.2% (250 mA/cm ²)	S4
Ni _{0.88} Fe _{0.18} O-1	340	49	Eret= 98.2% (10 mA/cm ²)	S5
Fe: Ni 40:60	340	57	The exact numerical values are not provided.	S6
NiFe LDH@NCP/NF	281	68	Overpotential change from 281 to 284 mV (by 1.07%), at 100 mA/cm ² for 40 h	S7

η – overpotential, TS – Tafel slopes, Eret – and potential retention, Jret – current density retention, Deg – degradation rate

References

- ^{S1} Acharya, P., Nelson, Z. J., Benamara, M., Manso, R. H., Bakovic, S. I. P., Abolhassani, M., ... & Greenlee, L. F. (2019). Chemical structure of Fe–Ni nanoparticles for efficient oxygen evolution reaction electrocatalysis. *ACS omega*, 4(17), 17209-17222.
- ^{S2} Gao, L., Tang, C., Liu, J., He, L., Wang, H., Ke, Z., ... & Xiao, X. (2021). Oxygen vacancy-induced electron density tuning of Fe₃O₄ for enhanced oxygen evolution catalysis. *Energy & Environmental Materials*, 4(3), 392-398.
- ^{S3} Zang, Y., Zhang, H., Zhang, X., Liu, R., Liu, S., Wang, G., ... & Zhao, H. (2016). Fe/Fe₂O₃ nanoparticles anchored on Fe-N-doped carbon nanosheets as bifunctional oxygen electrocatalysts for rechargeable zinc-air batteries. *Nano Research*, 9, 2123-2137.
- ^{S4} Zhang, G., Li, Z., Zeng, J., Yu, L., Zuo, C., Wen, P., ... & Qiu, Y. (2022). Ferric ions leached from Fe-based catalyst to trigger the dynamic surface reconstruction of nickel foam for high-efficient OER activity. *Applied Catalysis B: Environmental*, 319, 121921.
- ^{S5} Shi, G., Arata, C., Tryk, D. A., Tano, T., Yamaguchi, M., Iiyama, A., ... & Kakinuma, K. (2023). NiFe Alloy Integrated with Amorphous/Crystalline NiFe Oxide as an Electrocatalyst for Alkaline Hydrogen and Oxygen Evolution Reactions. *ACS omega*, 8(14), 13068-13077.
- ^{S6} Mirabella, F., Müllner, M., Touzalin, T., Riva, M., Jakub, Z., Kraushofer, F., ... & Diebold, U. (2021). Ni-modified

Fe₃O₄ (001) surface as a simple model system for understanding the oxygen evolution reaction. *Electrochimica Acta*, 389, 138638.

⁵⁷ Chen, X., Yu, X., Yang, C., & Wang, G. (2024). Enhancing OER and overall water splitting performance of amorphous NiFe LDH grown on Ni foam with the needle-like NiCoP transition layer. *Journal of Solid State Chemistry*, 333, 124649.